

Electron Extraction Dynamics in CdSe and CdSe/CdS/ZnS Quantum Dots Adsorbed with Methyl Viologen

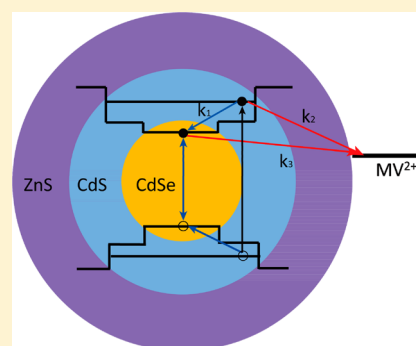
Ya-Feng Wang,^{†,‡} Hai-Yu Wang,^{*,†} Zheng-Shun Li,[†] Jia Zhao,[†] Lei Wang,[†] Qi-Dai Chen,[†] Wen-Quan Wang,[‡] and Hong-Bo Sun^{*,†,‡}

[†]State Key Laboratory on Integrated Optoelectronics, College of Electronic Science and Engineering, Jilin University, 2699 Qianjin Street, Changchun 130012, China

[‡]College of Physics, Jilin University, 2699 Qianjin Street, Changchun 130023, China

S Supporting Information

ABSTRACT: Semiconductor quantum dots (QDs) composed of multiple components are playing an important role in solar energy conversion as light harvesting materials. Electron extraction dynamics in CdSe and core/shell CdSe/CdS/ZnS colloidal QDs are studied by femtosecond transient absorption spectroscopy in this Article. Our study demonstrates that, in the presence of the commonly used electron acceptor, methyl viologen (MV^{2+}), electrons in the 1S state of CdSe QDs can be effectively extracted with a time constant less than 150 fs. With regard to type I core/shell CdSe/CdS/ZnS QDs, 400 nm excitation will mainly populate the CdS first, due to its large absorption cross section at around that wavelength. Electrons from the conduction band of CdS then can be directly extracted by MV^{2+} before transferring to core CdSe. Therefore, MV^{2+} can serve as an efficient bridge to extract electrons from the shell of type I QDs. As compared to the bare QDs, core/shell QDs have slower charge separation and much slower recombination rates. Thus, the core/shell QDs are beneficial for designing solar cells.



INTRODUCTION

Semiconductor quantum dots (QDs) have been widely explored due to their novel properties. These include their size-dependent bandgap, discrete conduction and valence bands, high photostability, and high photoluminescent quantum yield.^{1–9} These properties make it different from bulk semiconductors and result in its popularity in solar cell research.^{4,6} As a promising candidate for efficient, low-cost photovoltaic devices, quantum dot solar cells (QDSC) have a theoretical power conversion efficiency of as high as 66%.¹⁰ The mechanism of light-to-electrical energy conversion in QDSC is considered to be controlled by a series of charge-transfer processes, such as charge separation, hot electron extraction, multiple exciton generation (MEG), and plasmonic effects.^{11–17} Among these processes, the charge separation plays an important role in optimizing device performance.¹⁸ It is known that photoelectrons are generated when QDs are excited by photons whose energies are larger than the bandgap and subsequently recombine on a nanosecond time scale with a significant amount of irreversible energy loss.^{18–21} To alleviate this loss, several methods have been developed, such as capping QDs with shells or strongly coupling QDs to other semiconductor like TiO_2 .^{22–24} The investigation of charge transfer dynamics is helpful in the design of solar cells.^{18,25,26} Femtosecond transient absorption (TA) provides an ideal way to study the ultrafast dynamics. Previous ultrafast spectroscopy studies demonstrated that the electron relaxation

is related to surface states, capping, or core–shell structure.^{2,14,23,27,28}

However, despite the high quantum efficiency of QDs, charge separation efficiency and hence rapid extraction are of great importance in solar cells. Yet electron extraction dynamics have not been fully investigated. To conduct our experiment, CdSe QDs and core/shell CdSe/CdS/ZnS QDs were made and adsorbed with a widely used electron acceptor, methyl viologen (MV^{2+}). The core/shell QDs used here are type I alignment, as both the conduction band (CB) and the valence band (VB) edges of the core CdSe locate within the band gap of CdS.^{29,30} Because the bandgap of these CdSe QDs is about 2.1 eV, photons with energy monitored at 3.1 eV can pump the electrons into the $1P_e$ state, which then relax to the $1S_e$ state on a femtosecond time scale. With regard to core/shell CdSe/CdS/ZnS QDs, 3.1 eV pump light will mainly pump the CdS first, then the electrons will transfer to CdSe. We hope to find out whether the extraction of MV^{2+} electron from CdS is direct or not. Originally, the comparison between dynamics of CdSe QDs and CdSe– MV^{2+} complexes was provided to show the valid electron transfer (ET) process. Subsequently, the same view between CdSe/CdS/ZnS QDs and CdSe/CdS/ZnS– MV^{2+} complexes is given to testify the transfer process.

Received: March 11, 2014

Revised: June 16, 2014

Published: June 17, 2014

EXPERIMENTAL SECTION

Materials. Cadmium oxide (CdO, 99%), 1-hexadecylamine (HDA, 99%), tri-*n*-octylphosphine (TOP, 90%), tri-*n*-octylphosphineoxide (TOPO, 99%), Se powder (98%), oleic acid (OA, 90%), and octadecene (ODE, 90%) were purchased from Aldrich and used as received without further purification.

Synthesis of CdSe QD. Highly fluorescent CdSe nanocrystals were made according to a procedure modified from one that was used in previous report.³¹ For a reaction, the mixture of 677.9 mg of OA, 77.04 mg of CdO, and 8.1 g of ODE in a three-neck flask was heated to 280 °C for 20 min in a N₂ atmosphere until the mixture became clear. After this the solution was cooled to room temperature, and 1.5 g of TOPO and 1.5 g of HDA were added into the solution. It was then heated to 280 °C with vigorous stirring in N₂ atmosphere. At this temperature, 2.9 g of TOP-Se (10 wt %) and 1.1 g of ODE mixture were injected into the flask. The growth temperature was then reduced to 250 °C for 1 h to form homogeneous CdSe QDs. This reaction generated CdSe nanocrystals of about 3.4 nm in size. The reaction mixture was allowed to cool to room temperature, and an extraction procedure was used to purify the nanocrystals from side products and unreacted precursors: The same volume of toluene was added to the solution to isolate the QDs. A large amount of methanol was subsequently added, followed by centrifugation at 5000 rpm for 10 min. One milliliter of chloroform and ≥10 mL of acetone were then added for a second centrifugation. The core/shell QDs were synthesized using methods in available literature.^{31–34} The CdSe/CdS/ZnS QDs contained bare CdSe, 2 layers of CdS, and 2 layers of ZnS. The QD concentration in the purified solution was calculated using Lambert–Beer's law, to be 1.91×10^{-5} mol/L (S11, Supporting Information).

The QD–MV²⁺ complexes were made as follows. MV²⁺ (5 mM) dissolved in methanol was added to the QD solution in chloroform. Because MV²⁺ is poorly soluble in chloroform, sonication ensured that it was well dispersed and finally adsorbed onto the QDs surface.

Transmission Electron Microscopy (TEM) Measurements. TEM images of CdSe and CdSe/CdS/ZnS were produced on a JEM-2100F transmission electron microscope operating at an accelerating voltage of 200 kV. Figure 1 shows representative TEM images of initial CdSe core, core/shell QDs. The mean radii of the CdSe core and core/shell QDs are, respectively, 3.4 ± 0.4 and 5.6 ± 0.5 nm. The lattice planes extend straight across the particles, implying that the growth of shells occurs in the regime of coherent epitaxy.

Femtosecond Transient Absorption Spectrometer.^{35–38} A regeneratively amplified Ti:sapphire laser system (Spectra Physics, 800 nm, 100 fs, 1 mJ/pulse, and 250 Hz repetition rate) was used as the light source. The 800 nm output pulse from the amplifier was split into two parts to generate pump and probe pulses. The pump pulse at 400 nm was generated by the frequency doubling of a 800 nm pulse with a beta barium borate (BBO) crystal. The pump pulses at 567 and 580 nm were generated through the TOPAS system (Light Conversion). The energy of the 400 nm pump pulse was controlled by a variable neutral-density filter wheel. A white light continuum (from 440 to 700 nm) probe pulse was generated by attenuating and focusing the other 800 nm pulse into a sapphire window. The pump and probe beams were spatially overlapped at the sample (2 mm cuvette) with crossing areas of 500 and 300 μm in diameter, respectively. The

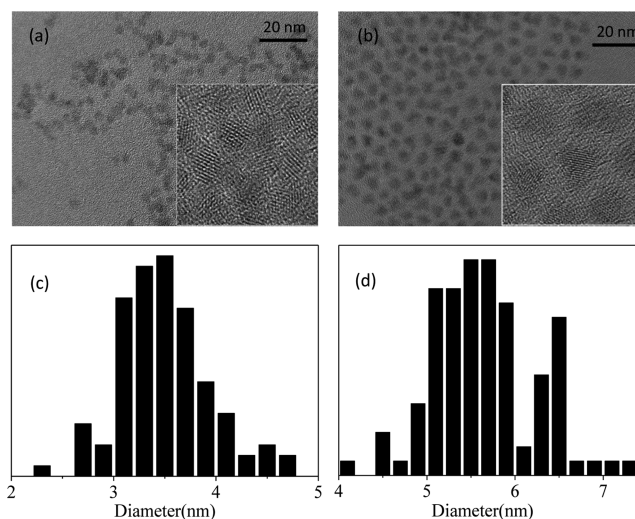


Figure 1. Transmission electron micrographs of (a) bare CdSe QDs and (b) CdSe/CdS/ZnS QDs. Size histogram of (c) bare CdSe QDs and (d) CdSe/CdS/ZnS QDs, measuring over 150 particles in each sample.

excitation energy density was adjusted to ~120 nJ/pulse (400 nm) and ~30 nJ/pulse (567 and 580 nm). The laser noise can be eliminated by comparing with the adjacent laser pulses (using a mechanical chopper to half the pump pulse frequency). Time-resolved transient absorption spectra were recorded with a highly sensitive spectrometer (Avantes AvaSpec-2048×14). The dynamics traces were obtained by controlling the relative delay between the pump and probe pulses with a stepper-motor driven optical delay line (Newport M-ILS250CC). The group velocity dispersion of the whole experimental system was compensated by a chirp program. The experimental data were fitted with a locally written program running in Matlab based on the proposed model. The instrument response function was measured using a quartz crystal instead of a sample pumped at 400 and 567 nm, respectively. All of the measurements were performed at room temperature.

RESULTS AND DISCUSSION

MV²⁺ was chosen as the electron acceptor for the following reasons. First, the reduction potential of MV²⁺ is located slightly below the conduction band edge of CdSe QDs; therefore, electrons from CdSe can transfer to MV²⁺ easily.^{39–42} Second, the absorption band of MV⁺ radical, at ~600–700 nm, is well separated from the QD absorption, allowing unambiguous distinction between it and the QD, as well as being convenient to observe.⁴¹ Third, MV²⁺ anchored to QDs have been studied extensively due to their ultrafast exciton dissociation, which occurs on a subpicosecond time scale.^{39,40,43} All of these properties make MV²⁺ a suitable electron acceptor for our experiment. The QD-to-MV²⁺ molar ratios must be maintained for different samples. Here, it is 1:7 for both (see Supporting Information S12 for a detailed discussion).

Figure 2 shows the optical absorption spectra of CdSe QDs and core/shell CdSe/CdS/ZnS QDs with and without MV²⁺. The static-state ultraviolet and visible (UV–vis) absorption spectrum of CdSe QDs exhibits a main peak at ~567 nm, which is assigned to the $1S_{3/2h}-1S_e$ excitonic transition. There is also a larger intensity bulk-like continuous absorption band with an onset at 400 nm. Because MV²⁺ shows no absorption at 300–700 nm, the CdSe–MV²⁺ complexes have the same

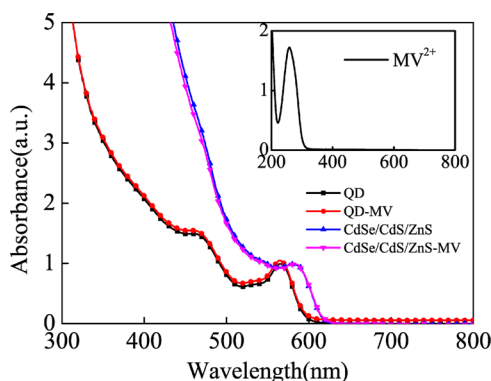


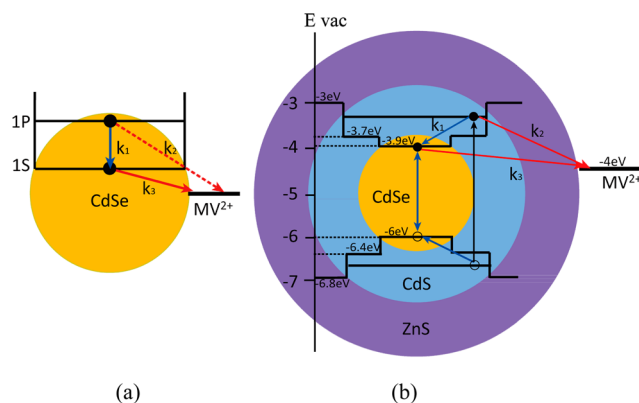
Figure 2. Normalized UV-vis absorption of bare CdSe QDs (■), QD-MV²⁺ complexes (red ●), CdSe/CdS/ZnS core/shell QDs (blue ▲), and CdSe/CdS/ZnS-MV²⁺ complexes (pink ▼). The inset shows the absorption of MV²⁺.

absorption as the free CdSe colloid in this range.⁴¹ In contrast to the CdSe QD, there is a red-shift of 20 nm in the absorption spectrum of core/shell QD caused by the CdS shell. The absorption at 400 nm is much larger than that of the bare CdSe, due to the big absorption cross section of CdS.^{44,45}

The time-resolved TA spectra at 2 ps of CdSe QDs and CdSe-MV²⁺ QDs are shown in Figure 3. Figure 3a,b is excited at 400 and 567 nm, respectively. The whole TA from 0 to 1.3 ns is shown in Supporting Information Figure S2. There is strong ground-state bleaching corresponding to the 1S exciton transition at 567 nm in Figure 3a and b. The bleaching magnitude of the QD-MV²⁺ complexes is much smaller than that of the bare QDs under the same conditions, which means that their populations must decrease. Hence, we ensure that the MV²⁺ extracts the electrons from QDs and turns into MV⁺ radicals. The transient spectra thus show a small absorption band at the range from 600 to 700 nm due to the absorption of

MV⁺ radicals (inset of Figure 3a and Supporting Information Figure S3b). Figure 3c compares the 650 nm dynamics of the bare QDs with that of the complexes. The difference clearly indicates the generation of MV⁺ radicals in the complexes. This may be attributed to the charge transfer from QDs to MV²⁺. As shown in Scheme 1a, the 400 nm pump light creates electrons

Scheme 1. Schematic Illustration of Electron Transfer in System of CdSe Adsorbed with MV²⁺ and Conduction and Valence Band Edge Positions (vs Vacuum)^a



^a(a) In CdSe-MV²⁺ complexes, k_1 is the state filling rate. k_2 and k_3 are the charge transfer rates. (b) In CdSe/CdS/ZnS-MV²⁺ complexes, k_1 is the rate of electrons transfer from CdS to CdSe. k_2 and k_3 are the charge transfer rates.

that populate the 1P_e level immediately; these electrons then relax to the 1S_e level on a femtosecond time scale. From 1S_e they will quickly transfer to MV²⁺. As a comparison, the experiments were performed by directly pumping at 567 nm. Figure 3b shows the TA spectra, and Figure 3d shows the 650 nm dynamics comparison. From these figures, we can see that

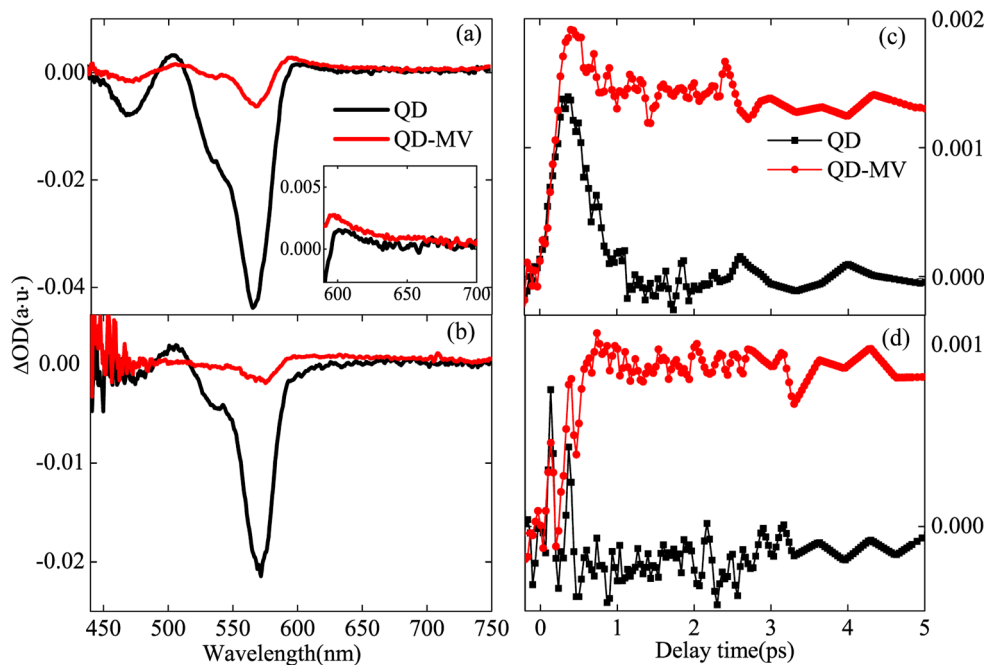


Figure 3. (a and b) Transient absorption spectra of CdSe at 2 ps excited at 400 and 567 nm. The solid black line is the TA of the bare QDs, and the red solid line is the QD-MV²⁺ complexes. Inset of (a) is the MV⁺ radical absorption at 600–700 nm. (c and d) Kinetics comparison at 650 nm pumped at 400 and 567 nm, respectively. ■, kinetics probed at 650 nm of the bare QDs; red ●, that of the complexes.

the results are similar to those from pumping at 400 nm. The 1S bleaching kinetics comparison is shown in Figure 4 ((a)

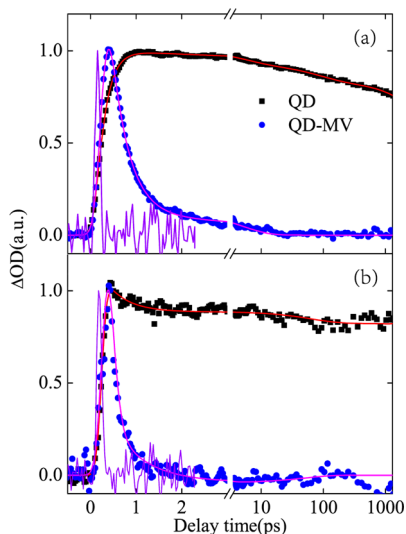


Figure 4. Kinetics comparison of CdSe QD and CdSe–MV²⁺ complexes, 1S bleaching of CdSe (■), absorption of MV²⁺ radicals (blue ●). (a) Kinetics excited at 400 nm. (b) Kinetics excited at 567 nm. Here, we monitored bleach at 580 nm to avoid the effect of excitation. Instrument response function (purple solid line).

excited at 400 nm and (b) excited at 567 nm). Interestingly, the 1S bleaching of the complexes arises much more quickly than does that of the bare CdSe QD. Rate constants need to be calculated to figure out the process. We use the rate equation below:

$$\begin{aligned} \frac{dN_{1p}}{dt} &= -k_1 N_{1p} - k_2 N_{1p} \\ \frac{dN_{1s}}{dt} &= k_1 N_{1p} - k_3 N_{1s} \end{aligned} \quad (1)$$

Assume there are three rate constants k_1 , k_2 , k_3 , which are marked in Scheme 1a. k_1 is the state filling rate without MV²⁺, and k_2 and k_3 are the electron extraction rates from the 1P_e and 1S_e levels, respectively. N_{1p} and N_{1s} are the populations of the 1P_e and 1S_e levels, respectively. The normalized solution to this equation is given by

$$N_{1p} = e^{-(k_1+k_2)t}$$

$$N_{1s} = \frac{k_1}{k_1 + k_2 - k_3} [e^{-k_3 t} - e^{-(k_1+k_2)t}] \quad (2)$$

When the bare QDs are excited at 400 nm, the state filling time ($1/k_1$) can be obtained by fitting the formation kinetics of the 567 nm bleaching (rising part of the ■ in Figure 4a), which is about 360 fs (Table 1). When the QD–MV²⁺ complexes are excited at 567 nm, k_3 can be obtained by monitoring the bleaching kinetics at 580 nm (blue ● in Figure 4b). As the decay of the bleaching is too fast to be fitted, k_3 is suggested to be $1/150 \text{ fs}^{-1}$, which is very close to our system time response (the FWHM of the instrument response function (IRF) is about 150 fs). We will test two conditions. The first assumes that k_2 exists and $(k_1 + k_2) > k_3$. Under this condition, eq 2 will consist of two components. The first is the rising part ($(-k_1/(k_1 + k_2 - k_3)) e^{-(k_1+k_2)t}$), which has the rising rate of $(k_1 + k_2)$, and the second is the decay part ($(k_1/(k_1 + k_2 - k_3)) e^{-k_3 t}$), which has the decay rate of k_3 ($1/150 \text{ fs}^{-1}$). In fact, the rising part cannot be calculated as it is too fast for fitting; however, we can observe the decay part with a rate of $\sim 1/360 \text{ fs}^{-1}$ from the fitted data (blue ● and pink line in Figure 4a). This is not too fast for fitting, which does not match our experimental observation, and hence the condition $(k_1 + k_2) > k_3$ cannot be true. Instead, we now assume that $(k_1 + k_2) < k_3$, and the solution to formula 1 becomes

$$N_{1p} = e^{-k_1 t}$$

$$N_{1s} = \frac{k_1}{k_3 - k_1} [e^{-k_1 t} - e^{-k_3 t}] \quad (3)$$

Here, we ignore the rate constant k_2 , because the decay rate we fit is about $1/360 \text{ fs}^{-1}$, just equal to k_1 when $(k_1/(k_3 - k_1)) e^{-k_1 t}$ contributes to the decay part, while the rising part is beyond the resolution as $(-k_1/(k_3 - k_1)) e^{-k_3 t}$ contributes to the rising part. This is perfectly consistent with our fitted data in Table 1: the kinetics at 580 nm of CdSe–MV²⁺ only has a decay time around 360 fs. From this the charge transfer mechanics are clear. When MV²⁺ is adsorbed on CdSe QD, electrons that cool to 1S_e from the 1P_e level will instantaneously transfer to MV²⁺ with a rate of around 150 fs. The decrease of the initial 1S_e population is a result of the charge transfer rate k_3 being over 2.4 times larger than the state filling rate k_1 . This means that electrons have already been extracted by MV²⁺ before they remain in the 1S_e level for a sufficient period of time, making the maximum bleaching value smaller.

To further investigate the dynamics of the charge transfer process, we choose type I CdSe/CdS/ZnS core/shell QDs. The

Table 1. Best-Fit Parameters of 1S Absorption Bleach Transients and MV²⁺ in Two Complexes with Function $I \propto \sum_i A_i \exp(-t/\tau_i)$ ^a

	excitation (nm)	τ_1 (ps)	τ_2 (ps)	τ_3	τ_4
CdSe	400	0.36 ± 0.1 (-1)	2 ± 0.2 (0.14)	>5 ns	
	567		2 ± 0.2 (0.16)	>5 ns	
CdSe–MV ²⁺	400		0.36 ± 0.005 (1)		
CdSe/CdS/ZnS	400	0.71 ± 0.1 (-1)	80 ± 1.4 (0.34)	>5 ns	
	580		46.6 ± 3.2 (0.24)	>5 ns	
CdSe/CdS/ZnS–MV ²⁺	400	0.47 ± 0.1 (-1)	1.8 ± 0.2 (0.58)	22 ± 1.6 (0.18) ps	>2 ns
	580		1.5 ± 0.1 (0.64)	36 ± 3.8 (0.14) ps	>2 ns

^aFitting error and relative weights (A_i) are given in brackets.

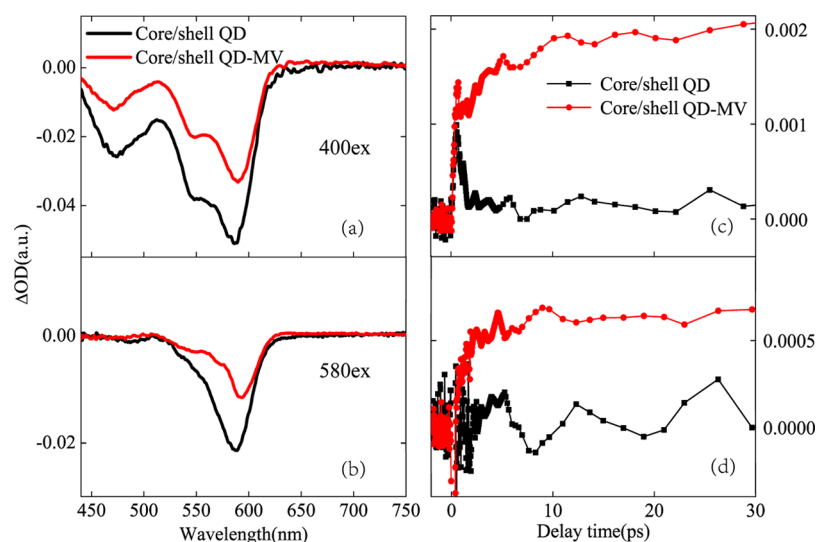


Figure 5. TA spectra at 2 ps of CdSe/CdS/ZnS and CdSe/CdS/ZnS–MV²⁺ complexes. (a) and (b) were pumped at 400 and 580 nm, respectively. The solid black line is the TA of the core/shell QDs, and the red solid line is the core/shell QD–MV²⁺ complexes. (c) and (d) show kinetics comparison probed at 660 nm pumped at 400 and 580 nm, respectively.

CdS shell functions as a tunneling barrier to slow the charge transfer or recombination. The growth of the outer ZnS shell provided better passivation of the surface states of CdS, as well as enhanced photostability and quantum yield.⁴⁶ Because of the wide band gap of ZnS, the charge transfer mechanism at the CdSe/CdS interface and the electron wave function delocalization into the CdS shell are not affected by the presence of the ZnS shell.⁴⁶ This kind of QD exhibits slow charge separation and recombination processes, making it easy to study charge transfer, which is well documented in the literature.^{11,12,23,47,48}

Figure 5 shows the TA spectra at 2 ps of type I CdSe/CdS/ZnS QDs and CdSe/CdS/ZnS–MV²⁺ complexes excited at 400 nm (Figure 5a) and 580 nm (Figure 5b). The TA spectra are given in Supporting Information Figure S4. Both spectra show a strong 1S ground-state bleaching at 587 nm. The difference between the bare QDs and these core/shell QDs is that 400 nm will pump the CdS first, as it has a much larger absorption cross section than CdSe. Figure 2 clearly shows that the absorption at 400 nm is much larger than that of the bare QD. The bleaching of the complexes has a smaller amplitude due to the charge transfer process, which results from the generation of MV⁺ radicals. Figure 5c and d shows the kinetics of MV⁺ radicals probed at 660 nm. Other than for the bare QDs, the MV⁺ absorption here has a much slower rise time over 30 ps. We ascribe this phenomenon to the slow charge transfer, as the CdS and ZnS shells inhibit the transfer process. We compare the 580 nm kinetics excited at 400 and 580 nm, respectively, in Figure 6a and b, which shows that the 1S bleaching of the complexes rises and recovers faster than that of the bare core/shell QDs. We thus prove that electron extraction is present in the complex system. The formation of MV⁺ radicals as shown by the absorption at 600–700 nm (Supporting Information Figure S5b) can further confirm the electron extraction process. The fitted data are shown in Table 1 to do the further calculation. Scheme 1b will help to explain in detail, where k_1 is the ET rate from CdS to CdSe and k_2 and k_3 are the charge separation rates. When excited at 580 nm, only the core CdSe generates electron–hole pairs, so MV²⁺ extracts electrons only from CdSe with a rate k_3 . k_1 and k_2 do not exist in this case.

Here, we change formula 1 and its solution eq 2 to

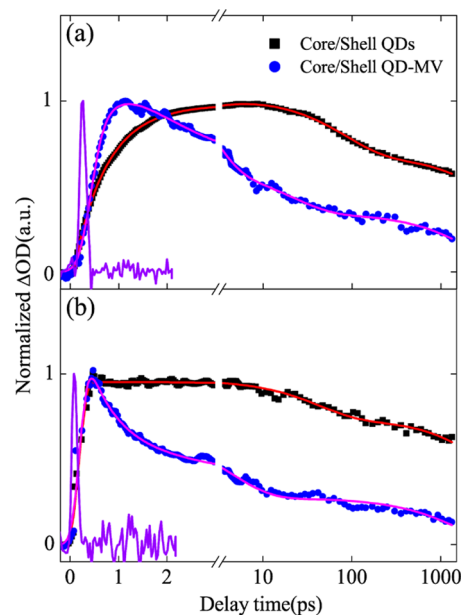


Figure 6. Kinetics comparison of CdSe/CdS/ZnS and CdSe/CdS/ZnS–MV²⁺, 1S bleaching of CdSe/CdS/ZnS (■), absorption of MV⁺ radicals (blue ●). (a) Kinetics excited at 400 nm. (b) Kinetics excited at 580 nm. Instrument response function (purple solid line).

$$\frac{dN_s}{dt} = -k_1 N_s - k_2 N_s$$

$$\frac{dN_c}{dt} = k_1 N_s - k_3 N_c \quad (4)$$

$$N_s = e^{-(k_1+k_2)t}$$

$$N_c = \frac{k_1}{k_1 + k_2 - k_3} [e^{-k_3 t} - e^{-(k_1+k_2)t}] \quad (5)$$

where N_s and N_c denote the population of the shell CdS and core CdSe, respectively. Under 400 nm excitation, the ET process from CdS to CdSe takes about 710 fs, indicating k_1 in

this system is $1/710 \text{ fs}^{-1}$. It does not matter whether the electron finally populates the $1P$ or $1S$ level of the core, because their energy difference is small as compared to the large gap between CdSe and CdS. Seen from Scheme 1b, k_3 can be obtained by fitting the 590 nm kinetics of CdSe/CdS/ZnS– MV^{2+} excited at 580 nm (blue ● in Figure 6b fitted in Table 1). k_3 is the fastest rate of the fitted data, $1/1.5 \text{ ps}^{-1}$. The value is consistent with the fitted data of the kinetics excited at 400 nm within error, which is about $1/1.8 \text{ ps}^{-1}$. The slower rates relate to the electron–hole recombination process. As the rising time constant of the bleaching is about 470 fs (blue ● in Figure 6a, fitted in Table 1), we know that $k_1 + k_2 = 1/470 \text{ fs}^{-1}$ using solution 2. The electron extraction rate k_2 can hence be calculated as $1/1.4 \text{ ps}^{-1}$, which is much slower than that of the CdSe– MV^{2+} complexes as expected. Figure 7 compares the

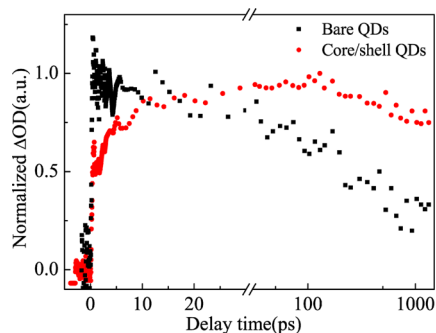


Figure 7. Charge recombination comparison of CdSe QDs (■) and core/shell QDs (red ●).

charge recombination process of CdSe– MV^{2+} and core/shell QD– MV^{2+} complexes. The process of the core/shell complexes extends to several nanoseconds, which is much slower than that of the bare QDs due to the CdS and ZnS shells. Because the shells contribute to the charge separation and prevent the charge recombination, they are of great potential application in solar cells. We conclude that about $1/3$ ($k_2/[k_1 + k_2]$) of the electrons from CdS can be extracted to MV^{2+} at a rate of $1/1.4 \text{ ps}^{-1}$ before they transfer to CdSe, thus accelerating the charge transfer process, which is significant to improve efficiency. Furthermore, the shells will certainly slow the recombination process, which is beneficial in the design of solar cells.

CONCLUSIONS

In summary, we have investigated the electron extraction dynamics of CdSe and core/shell CdSe/CdS/ZnS quantum dots (QDs) with MV^{2+} adsorbed on the surface by femto-second transient absorption spectrometer. We proved that the electrons in the $1S_e$ level of CdSe QDs can be efficiently extracted by MV^{2+} with a time constant less than 150 fs, while there are little electrons in $1P_e$ that transfer to MV^{2+} directly. The electrons extraction process is very different in core/shell CdSe/CdS/ZnS QDs. The electrons extraction time constants are slowed to 1.4 and 1.5 ps, from CdS and CdSe, respectively. The recombination is also slowed to several nanoseconds. We believe that the core/shell structure will be of potential application in solar cells. Also, if MV^{2+} or similar molecules are attached or linked to QDs as a bridge in quantum dot solar cells, electrons will be extracted efficiently.

ASSOCIATED CONTENT

Supporting Information

Additional calculations and figures, including the calculation for the molar concentration and the molar ratio, the whole TA spectra of CdSe QDs and core/shell QDs, and the absorption of MV^{2+} radicals for the two systems. This material is available free of charge via the Internet at <http://pubs.acs.org>.

AUTHOR INFORMATION

Corresponding Authors

*E-mail: haiyu_wang@jlu.edu.cn.

*E-mail: hbsun@jlu.edu.cn.

Notes

The authors declare no competing financial interest.

ACKNOWLEDGMENTS

We would like to acknowledge the financial support from the 973 project (grant no. 2014CB921302), the Natural Science Foundation of China (NSFC grant nos. 21273096 and 61076054), and the Doctoral Fund Ministry of Education of China (grant no. 20130061110048).

REFERENCES

- (1) Klimov, V. I. Spectral and Dynamical Properties of Multiexcitons in Semiconductor Nanocrystals. *Annu. Rev. Phys. Chem.* **2007**, *58*, 635–673.
- (2) Sippel, P.; Albrecht, W.; Mitoraj, D.; Eichberger, R.; Hannappel, T.; Vanmaekelbergh, D. Two-photon Photoemission Study of Competing Auger and Surface-mediated Relaxation of Hot Electrons in CdSe Quantum Dot Solids. *Nano Lett.* **2013**, *13*, 1655–1661.
- (3) Kamat, P. V. Quantum Dot Solar Cells. The Next Big Thing in Photovoltaics. *J. Phys. Chem. Lett.* **2013**, *4*, 908–918.
- (4) Kongkanand, A.; Tvrdy, K.; Takechi, K.; Kuno, M.; Kamat, P. V. Quantum Dot Solar Cells. Tuning Photoresponse through Size and Shape Control of CdSe–TiO₂ Architecture. *J. Am. Chem. Soc.* **2008**, *130*, 4007–4015.
- (5) Pattantyus-Abraham, A. G.; Kramer, I. J.; Barkhouse, A. R.; Wang, X. H.; Konstantatos, G.; Debnath, R.; Levina, L.; Raabe, I.; Nazeeruddin, M. K.; Grätzel, M.; Sargent, E. H. Depleted-Heterojunction Colloidal Quantum Dot Solar Cells. *ACS Nano* **2010**, *4*, 3374–3380.
- (6) Nozik, A. J. Nanoscience and Nanostructures for Photovoltaics and Solar Fuels. *Nano Lett.* **2010**, *10*, 2735–2741.
- (7) MacDonald, B. I.; Martucci, A.; Rubanov, S.; Watkins, S. E.; Mulvaney, P.; Jasieniak, J. J. Layer-by-Layer Assembly of Sintered CdSe(x)Te_{1-x} Nanocrystal Solar Cells. *ACS Nano* **2012**, *6*, 5995–6004.
- (8) Huynh, W. U.; Dittmer, J. J.; Alivisatos, A. P. Hybrid Nanorod-Polymer Solar Cells. *Science* **2002**, *295*, 2425–2427.
- (9) Dohnalová, K.; Poddubny, A. N.; Prokofiev, A. A.; Boer, W. D.; Umesh, C. P.; Paulusse, J. M. J.; Zuilhof, H.; Gregorkiewicz, T. Surface Brightens up Si Quantum Dots: Direct Bandgap-like Size-tunable Emission. *Light Sci. Appl.* **2013**, *2*, e47.
- (10) Ross, R. T.; Nozik, A. J. Efficiency of Hot-Carrier Solar Energy Converters. *J. Appl. Phys.* **1982**, *53*, 3813–3818.
- (11) Huang, J.; Huang, Z. Q.; Yang, Y.; Zhu, H. M.; Lian, T. Q. Multipleexciton Dissociation in CdSe Quantum Dots by Ultrafast Electrontransfer to Adsorbed Methylene Blue. *J. Am. Chem. Soc.* **2010**, *132*, 4858–4864.
- (12) Boulesbss, A.; Issac, A.; Stockwell, D.; Huang, Z. Q.; Huang, J.; Guo, J. C.; Lian, T. Q. Ultrafast Charge Separation at CdS Quantum Dot/Rhodamine B Molecule Interface. *J. Am. Chem. Soc.* **2007**, *129*, 15132–15133.
- (13) Huang, J.; Huang, Z. Q.; Yang, Y.; Zhu, H. M.; Lian, T. Q. Photoinduced Ultrafast Electron Transfer from CdSe Quantum Dots to Re-bipyridylcomplexes. *J. Am. Chem. Soc.* **2008**, *130*, 5632–5633.

- (14) Pandey, A.; Guyot-Sionnest, P. Hot Electron Extraction from Colloidal Quantum Dots. *J. Phys. Chem. Lett.* **2010**, *1*, 45–47.
- (15) Schaller, R. D.; Klimov, V. I. High Efficiency Carrier Multiplication in PbSe Nanocrystals: Implications for Solar Energy Conversion. *Phys. Rev. Lett.* **2004**, *92*, 186601(1)–186601(4).
- (16) Yu, P.; Wen, X. M.; Lee, Y. C.; Lee, W. C.; Kang, C. C.; Tang, J. Photoinduced Ultrafast Charge Separation in Plexcitonic CdSe/Au and CdSe/Pt Nanorods. *J. Phys. Chem. Lett.* **2013**, *4*, 3596–3601.
- (17) Batabyal, S.; Makhali, A.; Das, K.; Raychaudhuri, A. K.; Pal, S. K. Ultrafast Dynamics of Excitons in Semiconductor Quantum Dots on a Plasmonically Active Nano-structured Silver Film. *Nanotechnology* **2011**, *22*, 195704(1)–195704(4).
- (18) Tisdale, W. A.; Williams, K. J.; Timp, B. A.; Norris, D. J.; Aydil, E. S.; Zhu, X. Y. Hot-Electron Transfer from Semiconductor Nanocrystals. *Science* **2010**, *328*, 1543–1547.
- (19) Shockley, W.; Queisser, H. J. Detailed Balance Limit of Efficiency of p-n Junction Solar Cells. *J. Appl. Phys.* **1961**, *32*, 510–519.
- (20) Nozik, A. J. Quantum Dot Solar Cells. *Physica E* **2002**, *14*, 115–120.
- (21) Nozik, A. J. Intraband Relaxation in CdSe Quantum Dots. *Annu. Rev. Phys. Chem.* **2001**, *52*, 193–231.
- (22) Guyot-Sionnest, P.; Shim, M.; Matranga, C.; Hines, M. Spectroscopy and Hot Electron Relaxation Dynamics in Semiconductor Quantum Wells and Quantum Dots. *Phys. Rev. B* **1999**, *60*, R2181–R2184.
- (23) Pandey, A.; Guyot-Sionnest, P. Slow Electron Cooling in Colloidal Quantum Dots. *Science* **2008**, *322*, 929–932.
- (24) Yang, Y.; Rodríguez-Córdoba, W.; Xiang, X.; Lian, T. Q. Multiple Exciton Generation and Dissociation in PbS Quantum Dot-Electron Acceptor Complexes. *Nano Lett.* **2012**, *12*, 303–309.
- (25) Klimov, V. I.; McBranch, D. W. Femtosecond IP-to-IS Electron Relaxation in Strongly Confined Semiconductor Nanocrystals. *Phys. Rev. Lett.* **1998**, *80*, 4028–4031.
- (26) Chuang, C. H.; Chen, X. B.; Burda, C. Femtosecond Time-resolved Hot Carrier Energy Distributions of Photoexcited Semiconductor Quantum Dots. *Ann. Phys.* **2012**, *525*, 43–48.
- (27) Kaniyankandy, S.; Rawalekar, S.; Verma, S.; Palit, D. K.; Ghosh, H. N. Charge Carrier Dynamics in Thiol Capped CdTe Quantum Dots. *Phys. Chem. Chem. Phys.* **2010**, *12*, 4210–4216.
- (28) Wang, L.; Wang, H. Y.; Fang, H. H.; Wang, H.; Yang, Z. Y.; Gao, B. R.; Chen, Q. D.; Han, W.; Sun, H. B. Universal Electron Injection Dynamics at Nanointerfaces in Dye-Sensitized Solar Cells. *Adv. Funct. Mater.* **2012**, *22*, 2783–2791.
- (29) Zhu, H.; Lian, T. Wave Function Engineering in Quantum Confined Semiconductor Nanoheterostructures for Efficient Charge Separation and Solar Energy Conversion. *Energy Environ. Sci.* **2012**, *5*, 9406–9418.
- (30) Ning, Z.; Tian, H.; Qin, H.; Zhang, Q.; Ågren, H.; Sun, L.; Fu, Y. Wave-Function Engineering of CdSe/CdS Core/Shell Quantum Dots for Enhanced Electron Transfer to a TiO₂ Substrate. *J. Phys. Chem. C* **2010**, *114*, 15184–15189.
- (31) Dabbousi, B. O.; Rodríguez-Viejo, J.; Mikulec, F. V.; Heine, J. R.; Mattoussi, H.; Ober, R.; Jensen, K. F.; Bawendi, M. G. (CdSe)ZnS Core-Shell Quantum Dots: Synthesis and Characterization of a Size Series of Highly Luminescent Nanocrystallites. *J. Phys. Chem. B* **1997**, *101*, 9463–9475.
- (32) Yu, W. W.; Qu, L.; Guo, W.; Peng, X. Experimental Determination of the Extinction Coefficient of CdTe, CdSe, and CdS Nanocrystals. *Chem. Mater.* **2003**, *15*, 2854–2860.
- (33) Li, J. J.; Wang, Y. A.; Guo, W. Z.; Keay, J. C.; Mishima, T. D.; Johnson, M. B.; Peng, X. G. Large-Scale Synthesis of Nearly Monodisperse CdSe/CdS Core/Shell Nanocrystals Using Air-Stable Reagents via Successive Ion Layer Adsorption and Reaction. *J. Am. Chem. Soc.* **2003**, *125*, 12567–12575.
- (34) Hines, M. A.; Guyot-Sionnest, P. Synthesis and Characterization of Strongly Luminescing ZnS-Capped CdSe Nanocrystals. *J. Phys. Chem.* **1996**, *100*, 468–471.
- (35) Wang, L.; Wang, H. Y.; Wang, Y.; Zhu, S. J.; Zhang, Y. L.; Zhang, J. H.; Chen, Q. D.; Han, W.; Xu, H. L.; Yang, B.; Sun, H. B. Direct Observation of Quantum-Confined Graphene-Like States and Novel Hybrid States in Graphene Oxide by Transient Spectroscopy. *Adv. Mater.* **2013**, *25*, 6539–6545.
- (36) Wang, L.; Wang, H. Y.; Gao, B. R.; Pan, L. Y.; Jiang, Y.; Chen, Q. D.; Han, W.; Sun, H. B. Transient Absorption Spectroscopic Study on Band-Structure-Type Change in CdTe/CdS Core-Shell Quantum Dots. *Quantum Electronics. IEEE J. Quantum Electron.* **2011**, *47*, 1177–1184.
- (37) Wang, L.; Wu, C. F.; Wang, H. Y.; Wang, Y. F.; Chen, Q. D.; Han, W.; Qin, W. P.; McNeill, J.; Sun, H. B. Internal Structure-mediated Ultrafast Energy Transfer in Self-assembled Polymer-blend Dots. *Nanoscale* **2013**, *5*, 7265–7270.
- (38) Wang, L.; Zhu, S. J.; Wang, H. Y.; Wang, Y. F.; Hao, Y. W.; Zhang, J. H.; Chen, Q. D.; Zhang, Y. L.; Han, W.; Yang, B.; Sun, H. B. Unraveling Bright Molecule-Like State and Dark Intrinsic State in Green-Fluorescence Graphene Quantum Dots via Ultrafast Spectroscopy. *Adv. Optical Mater.* **2013**, *1*, 264–271.
- (39) Matytilsky, V. V.; Dworak, L.; Breus, V. V.; BasChé, T.; Wachtveitl, J. Ultrafast Charge Separation in Multiexcited CdSe Quantum Dots Mediated by Adsorbed Electron Acceptors. *J. Am. Chem. Soc.* **2009**, *131*, 2424–2425.
- (40) Zhu, H. M.; Song, N. H.; Rodríguez-Córdoba, W.; Lian, T. Q. Wave Function Engineering for Efficient Extraction of up to Nineteen Electrons from One CdSe/CdS Quasi-Type II Quantum Dot. *J. Am. Chem. Soc.* **2012**, *134*, 4250–4257.
- (41) Watanobe, T.; Honda, K. Measurement of the Extinction Coefficient of the Methyl Viologen Cation Radical and the Efficiency of Its Formation by Semiconductor Photocatalysis. *J. Phys. Chem.* **1982**, *86*, 2617–2619.
- (42) Morris-Cohen, A. J.; Peterson, M. D.; Frederick, M. T.; Kamm, J. M.; Weiss, E. A. Evidence for a Through-Space Pathway for Electron Transfer from Quantum Dots to Carboxylate-Functionalized Viologens. *J. Phys. Chem. Lett.* **2012**, *3*, 2840–2844.
- (43) Zhu, H.; Lian, T. Enhanced Multiple Exciton Dissociation from CdSe Quantum Rods: The Effect of Nanocrystal Shape. *J. Am. Chem. Soc.* **2012**, *134*, 11289–11297.
- (44) Talapin, D. V.; Mekis, I.; Götzinger, S.; Kornowski, A.; Benson, O.; Weller, H. CdSe/CdS/ZnS and CdSe/ZnSe/ZnS Core-Shell-Shell Nanocrystals. *J. Phys. Chem. B* **2004**, *108*, 18826–18831.
- (45) Van Embden, J.; Jasieniak, J.; Mulvaney, P. Mapping the Optical Properties of CdSe/CdS Heterostructure Nanocrystals: The Effects of Core Size and Shell Thickness. *J. Am. Chem. Soc.* **2009**, *131*, 14299–14309.
- (46) Deka, S.; Quarta, A.; Lupo, M. G.; Falqui, A.; Boninelli, S.; Giannini, C.; Morello, G.; Giorgi, M. D.; Lanzani, G.; Spinella, C.; Cingolani, R.; Pellegrino, T.; Manna, L. CdSe/CdS/ZnS Double Shell Nanorods with High Photoluminescence Efficiency and Their Exploitation as Biolabeling Probes. *J. Am. Chem. Soc.* **2009**, *131*, 2948–2958.
- (47) Huang, J.; Mulfort, K. L.; Du, P.; Chen, L. X. Photodriven Charge Separation Dynamics in CdSe/ZnS Core/Shell Quantum Dot/Cobaloxime Hybrid for Efficient Hydrogen Production. *J. Am. Chem. Soc.* **2012**, *134*, 16472–16475.
- (48) Verma, S.; Kaniyankandy, S.; Ghosh, H. N. Charge Separation by Indirect Bandgap Transitions in CdS/ZnSe Type-II Core/Shell Quantum Dots. *J. Phys. Chem. C* **2013**, *117*, 10901–10908.